Isomerization of *n*-heptane over Ni–WO_x/SiO_2–Al_2O_3 catalysts. Effect of operating conditions, and nickel and tungsten loading

Y. Rezgui [a,*], M. Guemini [a], A. Tighezza [b], and A. Bouchemma [a]

[a] *Laboratoire de Recherche de Chimie, Université d'Oum El Bouaghi, BP 358 Route de Constantine, Oum El Bouaghi 04000, Algeria*
[b] *Department of Chemistry, College of Sciences, King Saud University, Saudi Arabia*

Received 14 August 2002; accepted 9 January 2003

Isomerization of *n*-heptane over Ni–WO_x/Al_2O_3–SiO_2 catalysts was carried out in a continuous flow fixed-bed reactor under atmospheric pressure. The first part of this study deals with the preparation of two series of catalysts (A and B) by the sol–gel method, while the second part deals with the isomerization of *n*-heptane. The principal objective of this study was to choose the catalyst giving the best isomer yield (di- and tri-branched ones) with optimum reaction conditions (reaction temperature, reduction temperature and time on stream). From the results obtained, the optimum nickel content was found to be 15 wt% and it seems that the incorporation of tungsten (B series) leads to a significant enhancement in the activity of the prepared catalysts. After running on stream for 100 min, the catalyst with 15% nickel and 10% tungsten (B4 catalyst) gives the best results (29% conversion and 70% selectivity) at 250 °C.

KEY WORDS: catalysts; gasoline; pollution; octane number; isomerization; *n*-heptane.

1. Introduction

New environmental regulations impose the elimination of regulated gasoline additives such as tetraethyl lead and the reduction of aromatic compounds because of their detrimental environmental effects [1], which may be accompanied by a loss in the octane number. Consequently there has been a sharp rise in the requirements for octane enhancement processes. Current gasoline formulations include oxygenates (e.g. MTBE) as octane boosters to compensate for the elimination of lead and the reduction in aromatics content [2–4]. Another potential solution is to isomerize the straight-chain paraffins, which are a major constituent in some crude oil fractions, with a low octane number, into their branched counterparts with a higher octane number, and then use the obtained product as a blending stock for gasoline obtained from reforming. Thus isomerization may be regarded as one of the main technologies of the petroleum refining industry.

As lower reaction temperatures yield a greater proportion of branched alkanes at thermodynamic equilibrium, the development of low-temperature isomerization catalysts assumes importance. In this respect, isomerization reactions are currently carried out very successfully using bifunctional supported platinum catalysts (reaction temperature 383–453 K [5]) [6–9]. Despite the higher yields of branched isomers owing to the lower temperatures of the process, these catalysts are very sensitive to poisons such as water or sulfur compounds, and can cause corrosion and pollution problems [10,11]. Thus it is of paramount importance to prepare and elaborate new environmentally benign catalysts which can replace these commercial catalysts (Pt supported on acidic alumina). In this respect, several catalysts families have been proposed: zeolites, silica–alumina, aluminum phosphate, heteropolyacids (KEGGIN or DAUSON structure), resins (Amberlyst, Nafion, etc.) [12] and recently sulfated zirconia and supported tungsten oxide acids [13–16].

The need to isomerize *n*-heptane, an important fraction of naphtha with a very low octane number (RON = 0), to mono-branched isomers (RON = 42–65) and preferentially to multi-branched isomers (RON = 80–112) is obvious. This reactant was chosen as a feed because its cracking occurs easily, making it possible to estimate correctly the isomerization/cracking selectivity of the catalysts.

In this study, we focus on an analysis of the catalytic properties of Ni–WO_x/SiO_2–Al_2O_3 catalysts for *n*-heptane isomerization. We mainly discuss the effects of the acid and metallic functions on the catalytic performance using Ni–WO_x/SiO_2–Al_2O_3 catalysts with various contents of nickel and tungsten oxide. We also examine other factors, such as reduction temperature, reaction temperature and time on stream, which can influence catalyst activity and selectivity.

2. Experimental

2.1. Catalyst preparation

Sol–gel methods have several promising advantages over common methods such as precipitation,

* To whom correspondence should be addressed.
E-mail: yacinereference@yahoo.com

1011-372X/03/0400-0011/0 © 2003 Plenum Publishing Corporation

Table 1
Ponderal composition of the different catalysts

Catalyst	Ponderal composition		SiO_2/Al_2O_3 ratio
	Ni	W	
A1	10	0	1.83
A2	12	0	1.83
A3	15	0	1.83
B1	12	8	1.83
B2	12	10	1.83
B3	15	8	1.83
B4	15	10	1.83
B5	15	30	1.83
B6	17	8	1.83
B7	17	10	1.83

impregnation, etc. In general, sol–gel synthesis offers better control over surface area, pore volume and pore size distribution [17–19]. Besides, the number of unit operations necessary for the preparation can be reduced providing a more reliable and reproducible synthetic method especially for mixed oxide catalysts [20]. From this point of view, we have used this method to prepare two catalysts series:

- A series, comprising three catalysts without tungsten with 10, 12 and 15 wt% of nickel, respectively, for A_1, A_2 and A_3 catalysts.
- B series, comprising seven catalysts denoted as B_1, B_2, ... B_7 with ponderal composition listed in table 1.

A series catalysts were obtained by mixing, under vigorous stirring, an aqueous solution of nickel nitrate ($Ni(NO_3)_2{\cdot}6H_2O$) preliminarily acidified by nitric acid (pH of the solution = 2) with the required amounts of sodium silicate (Na_2SiO_3) and aluminum sulfate ($Al_2(SO_4)_3{\cdot}18H_2O$) solutions. To exchange undesirable ions, such as Na^+, the prepared gel was activated, under reflux conditions in a thermostat, with ammonium sulfate (liquid to solid ratio of 30) at 60 °C over a period of 48 h (this unit operation was repeated several times), washed with hot water (60 °C), dried at 120 °C for 4 h and finally calcined at 500 °C for 5 h. A heating rate of 10 °C/min was used.

B series catalysts were prepared by mixing the required amounts of aluminum sulfate, sodium tungstanate and nickel nitrate. To the sol obtained, under vigorous stirring, an aqueous solution of sodium silicate was added. The gel prepared underwent the same unit operations (activation, washing and drying) as the gel prepared for A series catalysts. The obtained catalysts were calcined in the temperature range 300–600 °C for 5 h.

2.2. Hydrogen TPR analysis

The surface species reducibility was determined by temperature-programmed reduction (TPR) using an Ohkura TP 2002 S equipped with a thermal conductivity detector. An amount of 0.100 g of the catalyst was loaded in the TPR apparatus and pre-treated at 500 °C in an air flow for 3 h, cooled to room temperature followed by heating to 600 °C at a rate of 5 °C/min in a flow of 5 vol% hydrogen in argon.

2.3. Catalytic test

The *n*-heptane isomerization was performed at atmospheric pressure using a continuous flow fixed-bed quartz reactor, with an inner diameter of 10 mm, operated under isothermal conditions, and heated by a controlled temperature electrical oven. The reactor outlet passed through a sampling valve connected to a gas chromatograph. The operating conditions were:

- Mass of the catalyst: 1 g.
- Reaction temperature ranging from 150 to 300 °C with a step of 50 °C.
- Weight hourly space velocity (WHSV): 4/h.
- Hydrogen/hydrocarbon (H_2/*n*-heptane) molar ratio equal to 5.

3. Results and discussion

3.1. Effect of calcination temperature

The dependence of the catalyst activities on calcination temperature was investigated at a reaction temperature of 250 °C, for a time on stream of 1 h and at various reduction temperatures.

As shown in figures 1(a)–(d), whatever the reduction temperature, B7 is the only active catalyst at a calcination temperature of 300 °C (B3, B4 and B6 activities are lower than 1%). The catalytic activity of B series catalysts increased with calcination, passed through a maximum (525 °C for B3, 500 °C for B4 and 475 °C for B6 and B7) and then decreased. Calcination at 600 °C yielded the lowest activity. The catalyst activities were dependent on the calcination temperature as well as on the quantities of tungsten and nickel. The calcination temperatures showing the maximum activity are higher with less tungsten and nickel. Interaction of tungsten and nickel with the support surface seems to be strong when the active species are present in small amounts, similar to observations previously reported by Hino *et al.* [21] for their study on the isomerization of *n*-butane over ($WO_3/ZrO_2 + Pt/ZrO_2$) catalysts. Moreover, at a reduction temperature of 500 °C, B3 is slightly more active than the other catalysts, whatever the calcination temperature.

Finally, we note that the optimum calcination temperature is situated in the range 475–525 °C. From figure 1(e) we can establish that the conversion difference (DC%) between the maximum conversion of a catalyst and its conversion at a calcination temperature of

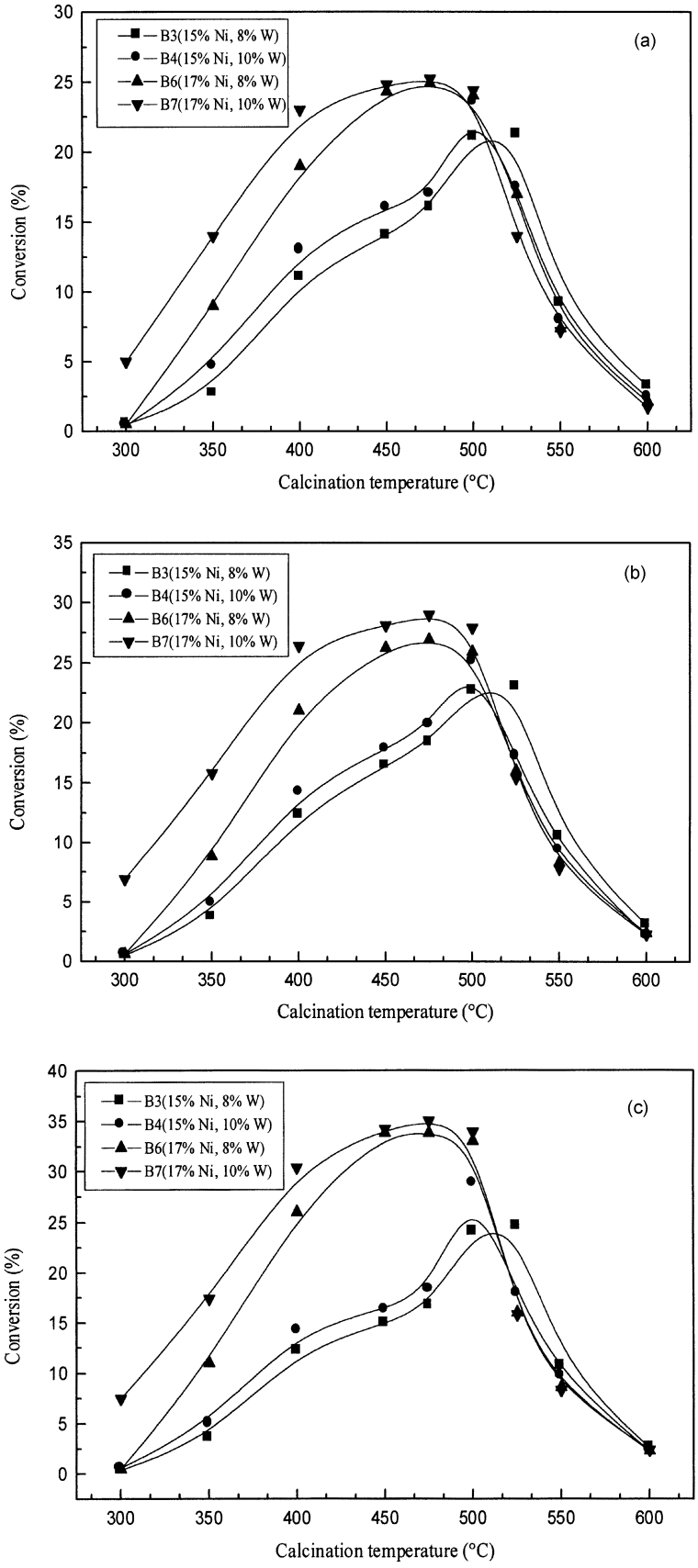

Figure 1. Effect of B series catalyst calcination temperature on activity. Reaction conditions: reaction temperature = 250 °C, time on stream = 1 h. (a) Reduction temperature = 300 °C, (b) reduction temperature = 400 °C, (c) reduction temperature = 440 °C, (d) reduction temperature = 500 °C. (e) Difference between conversion of B series catalysts at T_{cal} 500 °C and their conversion at the optimum calcination temperature and at the optimum reduction temperature.

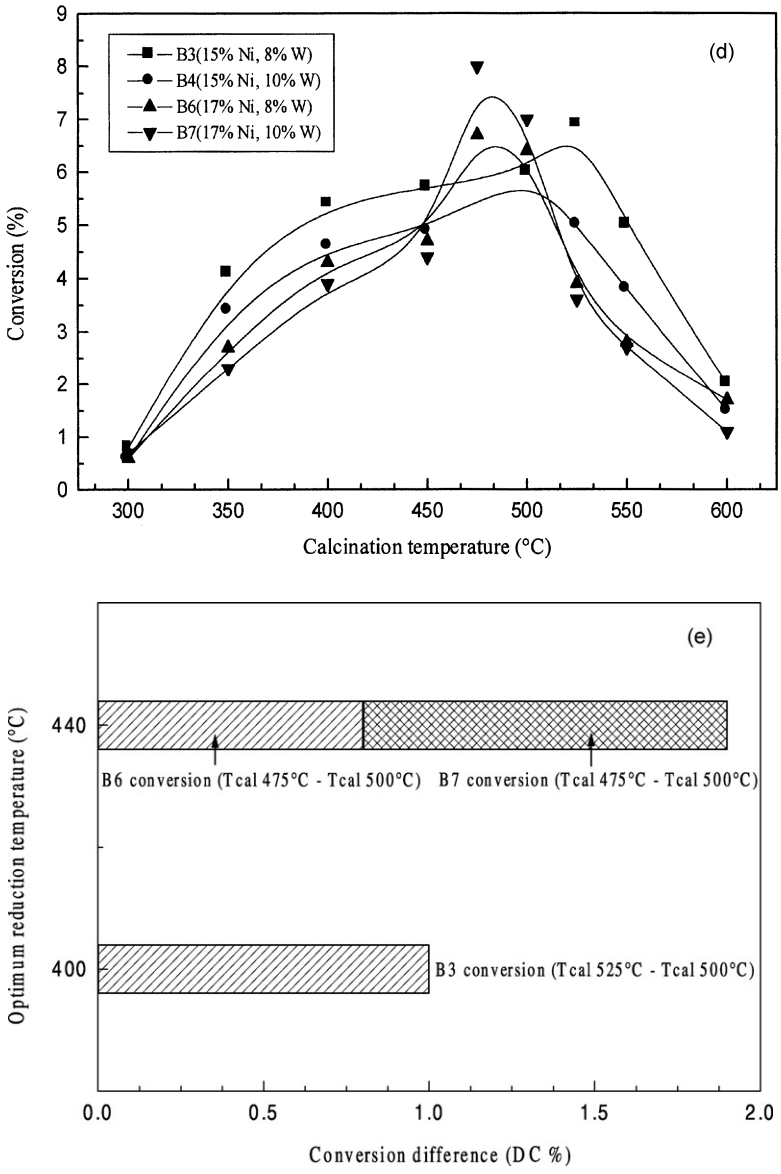

Figure 1. Continued.

500 °C (at the same reduction temperature) does not exceed 1.1%. With regard to this observation, we infer that 500 °C is the optimum calcination temperature for all the prepared catalysts, and thus we will deal only with the catalysts calcined at this temperature in the following discussion.

3.2. Reduction behavior

TPR patterns obtained for A3, B1, B2, B4 and B7 catalysts are presented in figure 2. The reduction of the catalyst free from tungsten (A3) shows a major consumption with a maximum at about 412 °C, which may be assigned to the reduction of NiO (the support cannot show any detectable peak at such a temperature). This reduction temperature is higher than that necessary for the reduction of the pure nickel oxide [22], which can be interpreted by an interaction between the nickel oxide and the silica–alumina (support). The same effect was observed in the case of the pyrolysis of gasoline selective hydrogenation catalysts and was interpreted in the same manner [23].

The TPR profiles obtained for B series catalysts are more complicated. The B1 catalyst exhibits a steady increase in the base line in the temperature range 300–390 °C, which may be due to the reduction of tungsten oxide species of various reducibilities, followed by two peaks centered around 440 and 480 °C. The low-temperature peak, by comparison with the A3 catalyst reduction and based on the fact that, in general, TPR profiles of the binary NiW catalysts appear as composite profiles of the corresponding monometallic ones, although somewhat modified by small shifts of the tungsten species reduction peak toward lower

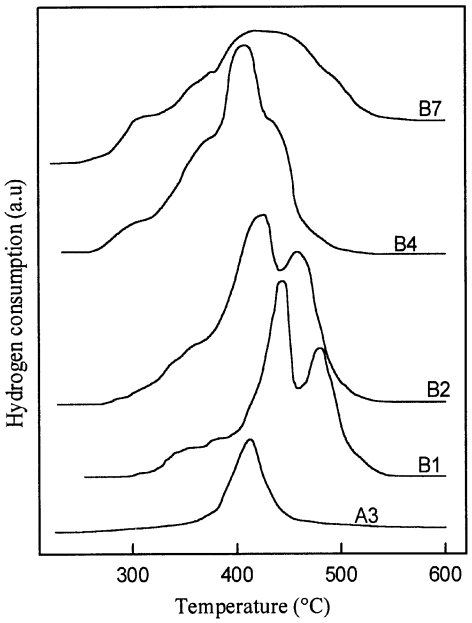

Figure 2. TPR profiles for A3, B1, B2, B4 and B7 catalysts.

temperatures and of the nickel species reduction peak toward higher temperatures, may be ascribed to the reduction of the nickel oxide (T_R (NiO) for A3 = 412 °C and T_R (NiO) for B1 = 440 °C) [24], while the high-temperature peak can be assigned to a further reduction of the tungsten oxide species. Similar features are observed in the profile of the B2 catalyst but the position of the peaks appears shifted toward a lower temperature by 20 °C. In the other hand, the B4 catalyst shows a steady increase in the base line in the temperature range 265–375 °C, a peak at about 410 °C and a shoulder at about 440 °C. The peak may be attributed to the reduction of NiO while the shoulder to a further reduction of the tungsten oxide species. In contrast to the previous three catalysts, the B7 catalyst displays an increase in the base line in the temperature range 260–375 °C and a very large peak centered at about 425 °C. This latter may be the result of the superimposition of two reduction peaks, the first of the NiO and the second of the WO_x species.

From the TPR profiles it appears that the peaks representing the reductions of nickel oxide and tungsten oxide shifted toward lower temperatures at higher tungsten loading, indicating that hydrogen reduction of these oxide species occurred more readily.

3.3. Effect of reduction temperature (T_R)

The effect of the catalyst reduction temperature on activity was studied at 250 °C over a duration of 100 min. As shown in figure 3, catalysts free from tungsten (A series) are inactive for T_R lower than 400 °C (activity equal to 0.5%). Their activities in the T_R range 400–475 °C increase with increasing amount of nickel (A_3 more active than A_2, which is itself more active than A_1) and remain constant in the range 475–600 °C. These results suggest that the activity level of these catalysts is related to prereduction temperature and to the amount of metallic nickel generated by hydrogen reduction. Hence, the presence of nickel, which possesses hydrogenating/dehydrogenating functions, is crucial to achieve high activity in a hydrogen flow.

The simultaneous presence of nickel and tungsten enhances the B series catalyst activity with respect to those of the A series catalysts whatever the reduction temperature. This activity increases with increasing reduction temperature and reaches a maximum at about 430 °C, then decreases to remain constant in the range 475–600 °C (figure 4). If we recall the TPR profiles,

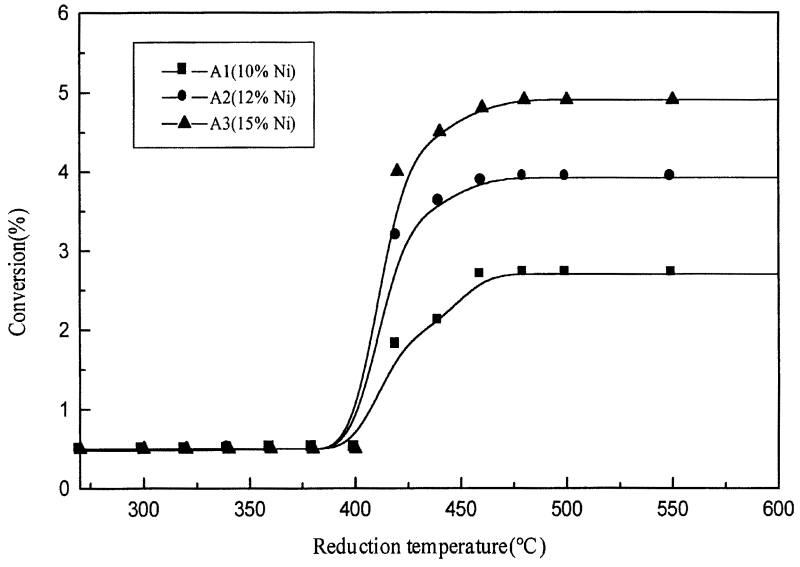

Figure 3. Effect of A series catalyst reduction temperature on activity. Reaction conditions: reaction temperature = 250 °C, time on stream = 100 min.

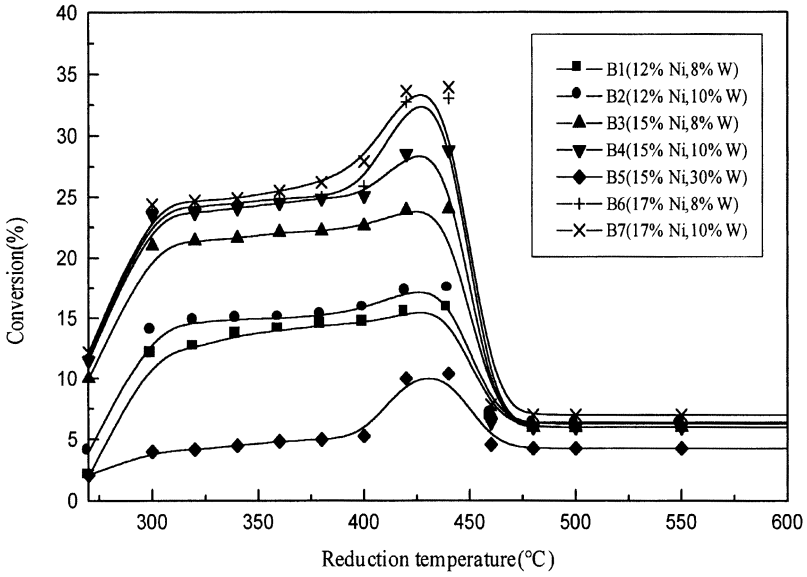

Figure 4. Effect of B series catalyst reduction temperature on activity. Reaction conditions: reaction temperature = 250 °C, time on stream = 100 min.

these results may be interpreted by the presence of reduced tungsten oxide species generated by hydrogen reduction, these reduced species being more active than the tungsten trioxide (WO_3) [25–28], and by a tungsten–nickel interaction which is translated by a shift in tungsten reduction temperatures toward lower values and those of the nickel toward higher ones. Above 430 °C the catalyst activity exhibits a decrease which may be due to the fact that higher reduction temperatures induce a large amount of undesirable tungsten (and support) reduction. The same result was reported by Larsen and Petkovic [29] with platinum supported on tungstated zirconia catalysts.

Since the B series catalysts are more active than the A series ones, we will deal only with the former in the following discussion.

3.4. *Effect of time on stream*

The effect of time on stream was studied at the optimum reduction temperature (430 °C) with the following operating conditions: $H_2/n\text{-}C_7 = 5$; weight hourly space velocity (WHSV) = 4/h.

As shown in figure 5, all the catalysts exhibited a decrease in their activity with increasing time on stream (TOS), the deactivation being more rapid during the first few minutes, and the activity remaining steady after 100 min without any further observable trend to deactivation. The deactivation rate was also more rapid at higher temperatures (figure 5(b)), the effect being dependent on the nickel content (it was more pronounced when the nickel content was low). This deactivation may be due mainly to the loss of the hydrogen dissociation capacity of WO_x species, which is rapidly deactivated by coke [30].

3.5. *Effect of nickel loading*

This effect was studied at 250 °C for a time on stream of 100 min and a reduction temperature of 430 °C.

As shown in figure 6, conversion increased with increasing nickel content, which may be due to the fact that the incorporation of nickel on catalysts produces a beneficial effect since it reduces the rate of deactivation and consequently increases the catalyst activity. Similar observations were reported by Yori and Parera [31] during their studies on the isomerization of *n*-butane over Ni/SO_4^{2-}–ZrO_2 and by Matsuda *et al.* [32] during their studies on the isomerization of *n*-heptane over molybdenum oxide catalysts where they confirmed that nickel was effective in preventing deactivation and consequently in enhancing catalyst activity. Selectivity to isomerization and isomerization/cracking (I/C) ratio increased with nickel content to reach a maximum at about 15% nickel then they decreased monotonically. Such a catalytic behavior can be explained by the fact that in the range 12–15% nickel the value of the metallic site/acid site function ratio is less than the optimal value for isomerization, thus increased metal function of the catalysts (nickel) prompts the formation of isomers via a reduction of the diffusion path between two metallic sites. Hence, the possibility that the intermediate species would encounter acid sites and would be cracked during its migration from one metallic site to another is also less. In contrast, in the range 15–17% nickel there are enough metallic sites to form olefins for feeding all the acid sites, and further increased metal function prevents the isomerization reaction and increases the rate of cracking and hydrogenolysis reactions (table 2) (nickel is an active component for the hydrogenolysis reaction [32]). Thus the observation of a maximum in the nickel content

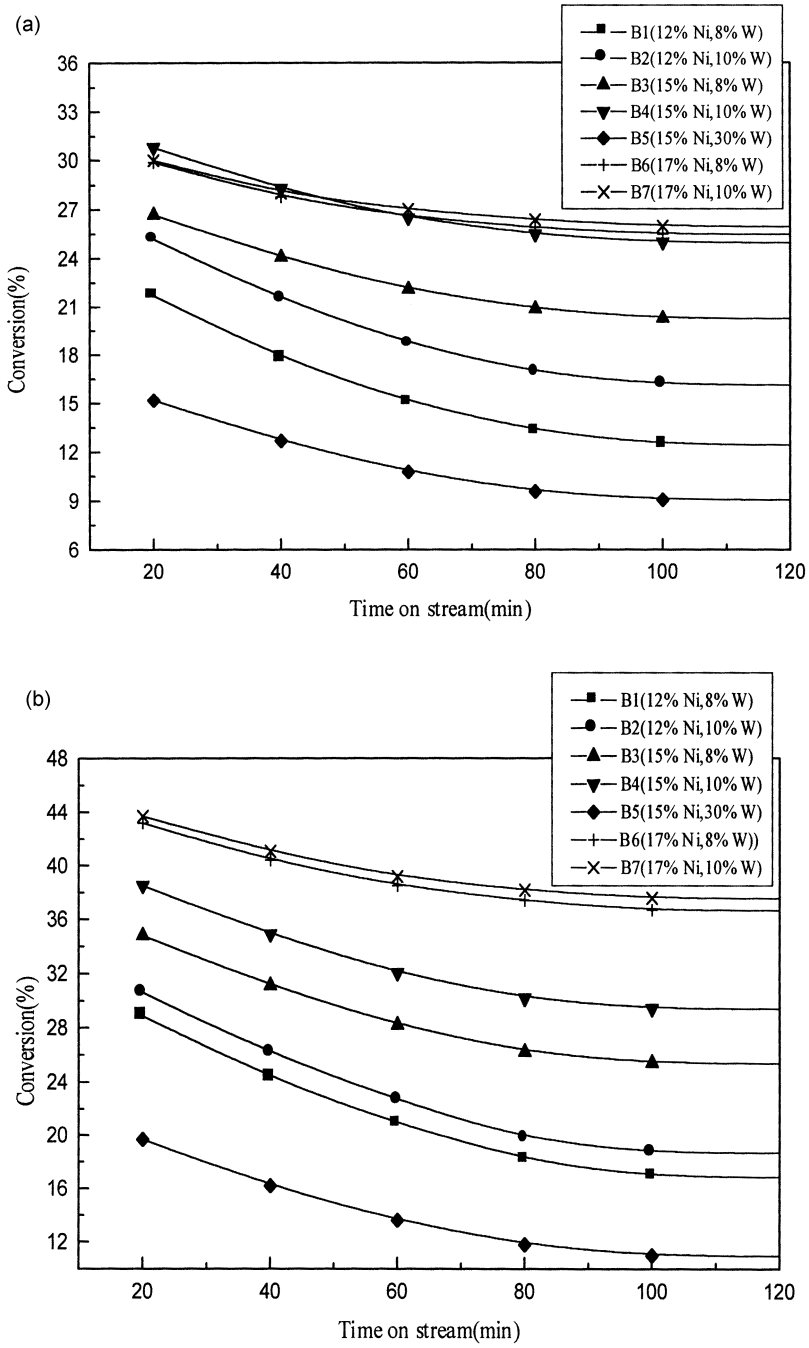

Figure 5. Effect of time on stream on B series catalyst activity for a reduction temperature of 430 °C: (a) reaction temperature = 150 °C; (b) reaction temperature = 300 °C.

proves that, in our case, the reaction proceeds via a bifunctional mechanism [33].

Another point of view may be taken where metallic nickel assures the formation of dissociated hydrogen necessary to generate active acid sites. The availability of the dissociated hydrogen is not only important for the generation of the acid sites but also for the elimination of ionic intermediates from the surface before β-scission events occur, avoiding cracking and polymerization reactions and thus increasing the isomerization selectivity. The same results were observed by Falco *et al.* [30] during their studies on the influence of platinum concentration on tungsten oxide-promoted zirconia during *n*-hexane isomerization.

When the nickel content exceeds a certain threshold (in our case 15%), the amount of hydrogenolysis gas is sufficient to increase the mass transfer resistance which causes an increase of the intermediate species residence time. Hence the possibility that these species could be cracked is greater.

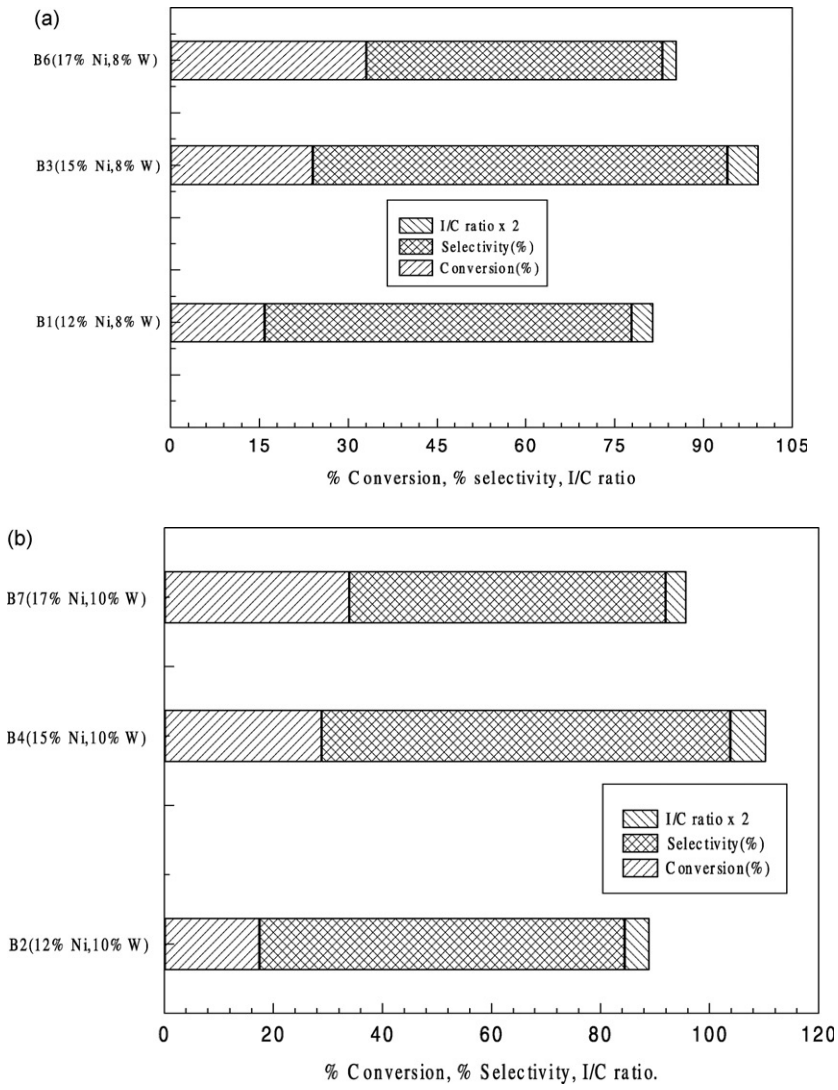

Figure 6. Effect of nickel loading on *n*-heptane isomerization over B series catalysts with (a) 8 wt% tungsten and (b) 10 wt% tungsten. Reaction conditions: reaction temperature = 250 °C, reduction temperature = 430 °C.

3.6. *Effect of tungsten loading*

The same operating conditions as those used in the case of nickel content were applied in this study.

As shown in figures 7(a)–(c), increasing the tungsten loading induces an increase in the activity of the catalysts. For 30% tungsten, a noticeable drop in the activity was observed. This effect may be due to poor tungsten

Table 2
Product distribution in the isomerization of *n*-heptane over B series catalysts

Catalyst	B2 (12% Ni)	B4 (15% Ni)	B7 (17% Ni)	Catalyst	B2 (12% Ni)	B4 (15% Ni)	B7 (17% Ni)
Conversion (%)	17.4	28.8	33.9	2,3 DMP (2,3-dimethylpentane)	3.5	3.9	3.8
Selectivity (%)				2,4 DMP (2,4-dimethylpentane)	3.6	4.0	4.3
Isomerization	67	75	58	3,3 DMP (3,3-dimethylpentane)	1.9	2.1	2.1
Cracking	29.78	23	30.42	2,2,3 TMB (2,2,3-trimethylbutane)	0.3	0.1	0.2
Cyclization	3.22	2	11.58	Cracking (hydrogenolysis) products			
Product distribution (%)				C_1	8.0	11.0	27.8
Isomerization products				C_2	9.4	8.9	7.7
2 MH (2-methylhexane)	44.5	42	42.8	C_3	25.0	22.1	14.9
3 MH (3-methylhexane)	41.7	43.3	42.1	C_4	28.6	27.4	16.1
3 EP (3-ethylpentane)	1.2	1.4	1.3	C_5	13.4	13.9	12.6
2,2 DMP (2,2-dimethylpentane)	3.3	3.2	3.4	C_6	15.6	16.7	20.9

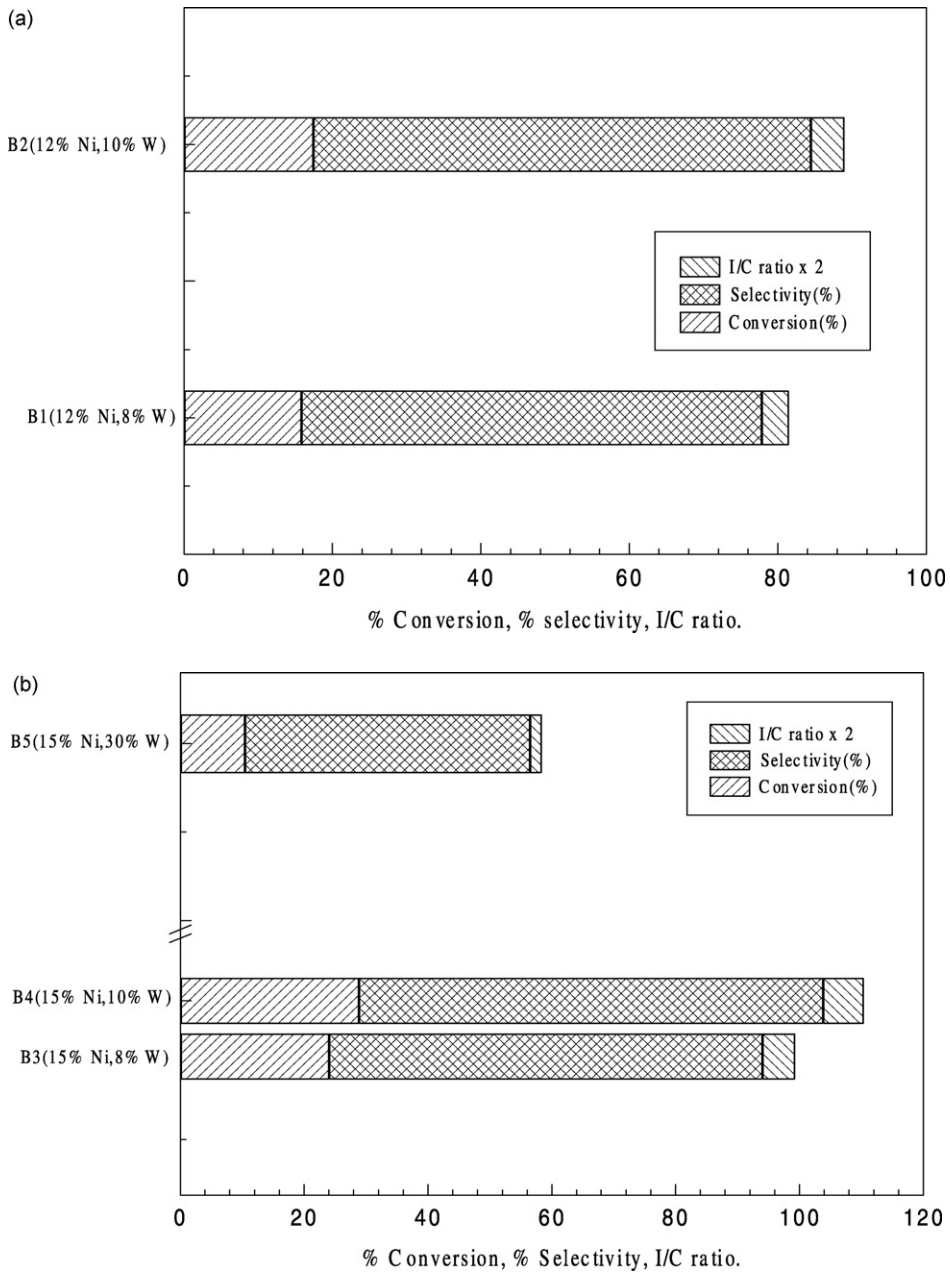

Figure 7. Effect of tungsten loading on *n*-heptane isomerization over B series catalysts. Reaction conditions: reaction temperature = 250 °C, reduction temperature = 430 °C. (a) 12 wt% nickel, (b) 15 wt% nickel, (c) 17 wt% of nickel. (d) Effect of tungsten loading on the B series catalyst (I/C) ratio difference.

repartition as a multilayer. Similar results were reported by Ouafi *et al*. [34] during their studies on the nature and the structure of tungsten surface species present on $NiO–WO_3/Al_2O_3$ hydrotreating catalysts, where they determined that the tungsten-like monolayer coverage limit was about 40% WO_3 and that bulk WO_3 was detected after this limit. The same effect was also mentioned by Benitez *et al*. [35] who reported that the WO_3 monolayer value for the WO_3/γ-Al_2O_3 system is between 24 and 30%. On the other hand, increasing the tungsten loading increased the isomerization selectivity and I/C ratio; this increase was more pronounced when the nickel content was high (figure 7(d), where $DR_3(R(B7) - R(B6)) > DR_2(R(B4) - R(B3)) > DR_1(R(B2) - R(B1))$: R is the I/C ratio). These results may be explained by:

- The reduced tungsten species' activity toward isomerization which can be attributed to their metallic character [25–27,36] or, if they are large enough, to their ability to stabilize carbenium ion intermediates by delocalization of the corresponding negative charge among several oxygen atoms [14,37,38].
- Oxygen atoms of WO_x species could bond dissociated hydrogen atoms formed in H_2 dissociation (by metallic nickel function) or C–H bond activation steps,

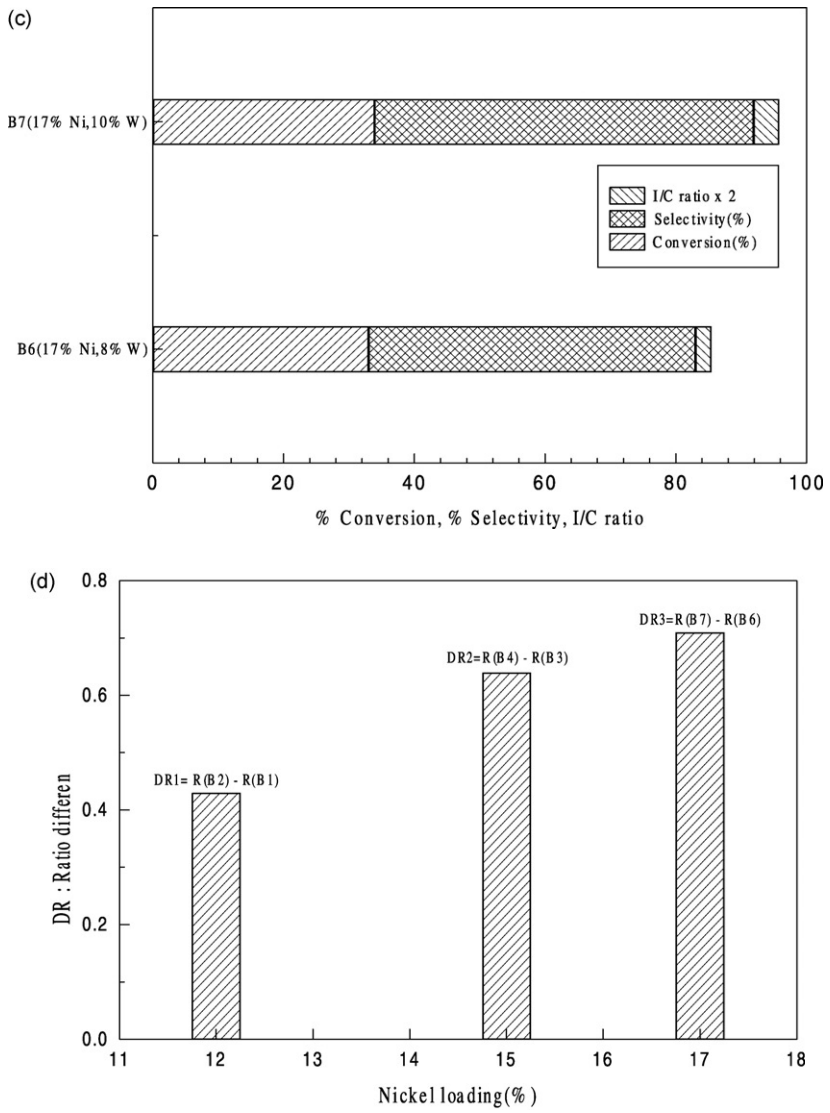

Figure 7. Continued.

consequently providing the Brønsted W–O_xH acidic sites and thus enhancing the rate of isomerization reaction [25,39,40].

- The presence of nickel is favorable for improving the tungsten dispersion in catalysts [34]. This phenomenon could explain the effect that, at the same tungsten loading, the isomerization level increases with increasing nickel content.
- It is believed that the surface residence time of carbenium ions is much shorter in the case of PtWZ catalysts (by comparison with PtSZ), thereby preventing β-fission reactions that lead to acid-catalyzed cracking [29,41]. This effect is related to the WO_x ($x \leq 2$) species that are also present in our catalysts.
- According to Meijers *et al.* [42], catalyst activity and stability are related to both Lewis and Brønsted acid sites. Addition of tungsten oxide increases the Brønsted site density at the expense of Lewis sites while maintaining the density of total sites constant [43]. It is known that Lewis sites catalyze favorably cracking reactions associated with the formation of coke [44]; thus addition of tungsten increases the catalyst selectivity to isomerization.

3.7. *Effect of SiO_2/Al_2O_3 ratio*

This study was carried out at 250 °C over Ni–WO_x/SiO_2–Al_2O_3 catalysts containing the same amount of nickel (15%) and tungsten (10%) but different SiO_2/Al_2O_3 ratios (1.83, 3, 5 and 7).

As shown in figure 8, an increase in the SiO_2/Al_2O_3 ratio induces a decrease in the activity. This decrease in conversion may be due to the decrease in available acid sites for the isomerization/cracking reactions. In catalysts with high SiO_2/Al_2O_3 ratios, the acid density is lower, so each intermediate olefin formed at a nickel dehydrogenating site comes into contact with very few acid sites between two nickel sites, which could favorably lead to the formation of isomerized products. In catalysts

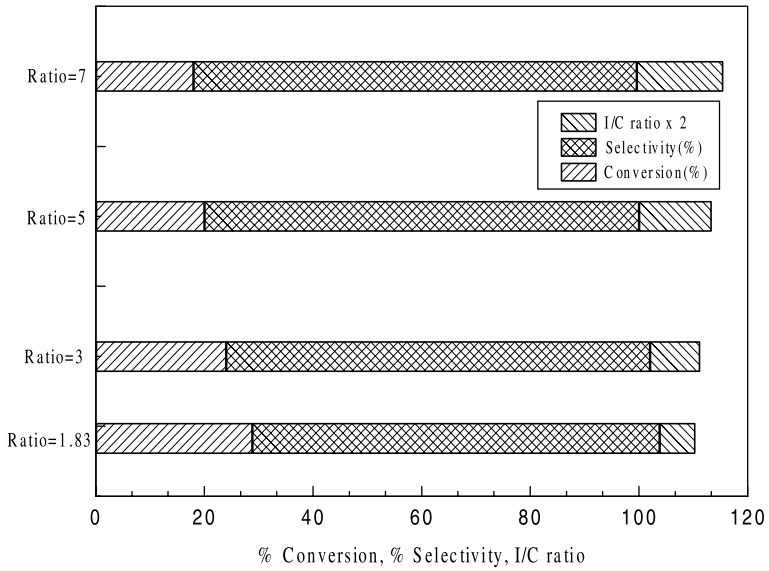

Figure 8. Effect of SiO_2/Al_2O_3 ratio on *n*-heptane isomerization over B series catalysts with 15 wt% nickel and 10 wt% tungsten. Reaction conditions: reaction temperature = 250 °C, reduction temperature = 430 °C.

with lower SiO_2/Al_2O_3 ratios, each intermediate olefin comes into contact with more acid sites between two nickel sites and thus the cracking tendency clearly predominates.

3.8. Effect of space velocity

The aim of this study was to find the reaction progress in time at optimum conditions for the chosen catalyst (B4). For this purpose, several reaction parameters were measured: the overall conversion, the yield of branched isomers, the yield of cracked products and the ratio of multi-/mono-branched isomers obtained. As mentioned, an important aspect of the present application is to limit the extent of cracking, and we know that these two reactions (isomerization and cracking) can proceed either simultaneously or consecutively:

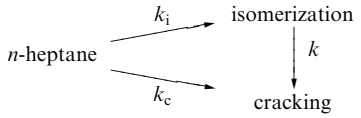

As isomerization reactions are faster than the cracking ones, a good catalyst will isomerize selectively until high conversions are reached, whereas a poor catalyst will crack even at low conversions.

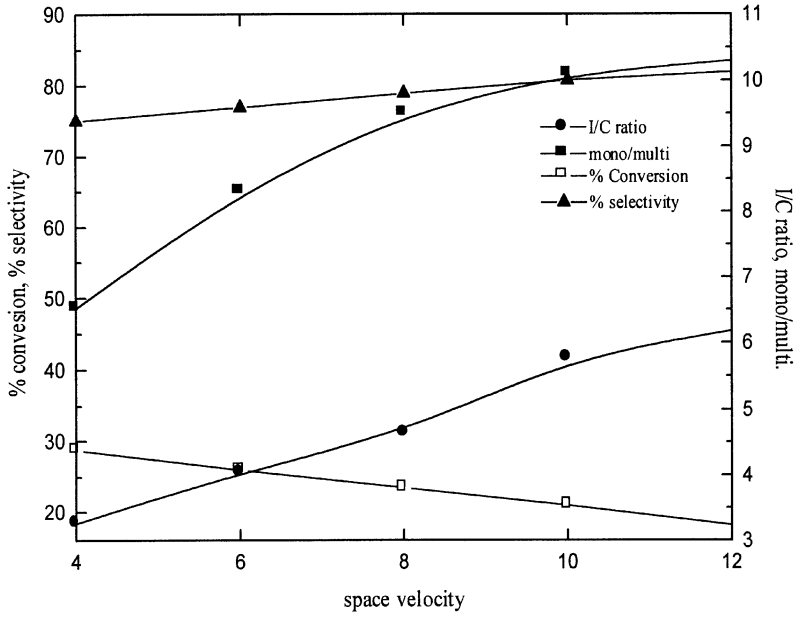

Figure 9. Effect of space velocity on *n*-heptane isomerization over the B4 catalyst. Reaction conditions: reaction temperature = 250 °C, reduction temperature = 430 °C.

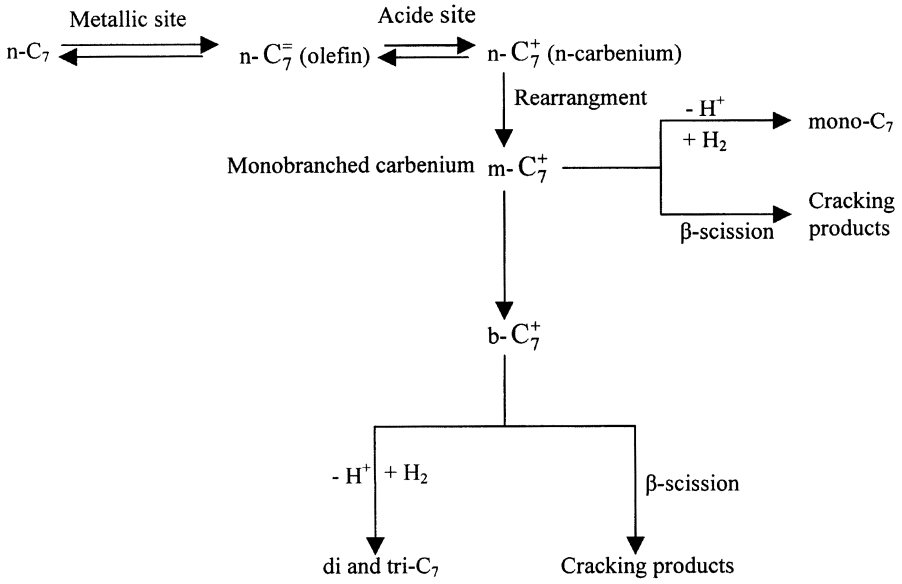

Scheme 1.

Our results (figure 9) indicate that an increase in the space velocity (a decrease in the contact time) leads to a decrease in conversion and an increase in the selectivity to isomers. The increase in the ratio of isomerized to cracked *n*-heptane (I/C) is a result of the decrease in cracking, which being slower than the isomerization reaction is less favored at higher space velocities (lower residence times). This result verifies that the formation of cracking products apparently succeeds the formation of branched isomers. Moreover, the ratio of mono- to multi-branched isomers (mono/multi) also increased with space velocity, namely with the conversion of *n*-heptane. This result indicates that the isomerization first leads to mono-branched isomers mainly, then to multi-branched ones. With regard to the above results, the mechanism of *n*-heptane transformation over Ni–WO_x/Al_2O_3–SiO_2 catalysts can be written as in scheme 1. A similar mechanism was suggested by Chao *et al.* [45] during their study on the hydroisomerization of light normal paraffins over series of platinum-loaded

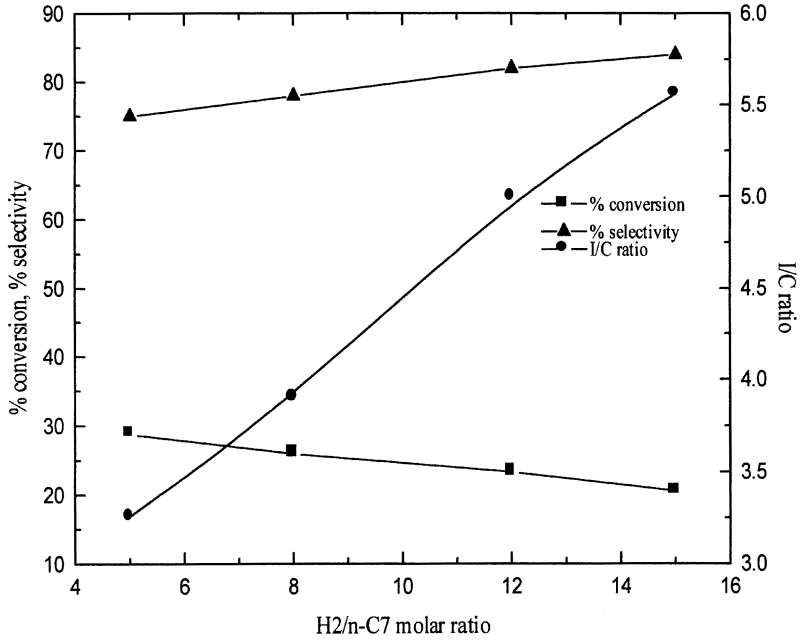

Figure 10. Effect of H_2/*n*-C_7 molar ratio on *n*-heptane isomerization over the B4 catalyst. Reaction conditions: reaction temperature = 250 °C, reduction temperature = 430 °C.

mordenite and beta catalysts (they considered both the classical bifunctional route and the dimerization cracking route).

3.9. Effect of H_2/n-C_7 molar ratio

The influence of changing the H_2/n-C_7 molar ratio on the conversion and I/C values was investigated at 250 °C by varying the hydrogen flow rate and keeping the partial pressure of *n*-heptane constant. As shown in figure 10, increasing the H_2/n-C_7 molar ratio from 5 to 15 decreased the conversion and increased the selectivity to isomers (I/C ratio increased). The decrease in conversion was probably due to an increase in the overall (n-$C_7 + H_2$) space velocity, while the increase in the I/C ratio could be due to the fact that isomerization reactions are faster than cracking reactions. Besides, as cracking of isoheptanes is faster than cracking of *n*-heptane, cracking reactions predominate at high conversions when iso-products are present in large amounts.

4. Conclusion

The results of the catalytic test reaction with pure C_7 feed indicate that, whatever the reduction temperature, catalysts with tungsten (B series) show improved catalytic activities as compared to those free from tungsten (A series). Furthermore, prereduction in hydrogen at 430 °C, the optimum reduction temperature, greatly increases the catalyst activity.

All B series catalysts deactivate with time on stream, with the conversion remaining steady after 100 min. On increasing the nickel loading, conversion increases as does selectivity to isomerization, which reaches a maximum and then decreases. Moreover, the presence of WO_x species enhances both activity and selectivity.

Furthermore, the results obtained for the prototype catalyst (B4: 15 wt% Ni and 10 wt% W) indicate that the hydrogen pressure, weight hourly space velocity and SiO_2/Al_2O_3 ratio strongly influence the reaction. At 250 °C, WHSV = 4/h and H_2/n-$C_7 = 5$, it has been reported that isomerization can be achieved with moderate selectivity (70%) at a conversion of 29%. The major reaction products were isomerization products (mainly 2 MH, 3 MH, 2,2 DMP, 2,3 DMP and 2,4 DMP) followed by cracking products (C_1–C_6) and a small amount of cyclization products.

In summary, it can be concluded that the system Ni–WO_x/SiO_2–Al_2O_3 exhibits interesting behavior as an isomerization catalyst.

Acknowledgment

The authors would like to acknowledge the contribution of Professors J.P. Saweresyn (Physicochimie des processus de combustion, University of Science and Technology of Lille, France) and E. Payen (Laboratory of Homogenous and Heterogenous Catalysis, University of Science and Technology of Lille, France).

References

[1] I.E. Maxwell and J.E. Naber, Catal. Lett. 12 (1992) 105.
[2] M.R. Gonzalez, K.B. Fogash, J.M. Kobe and J.A. Dumesic, Catal. Today 33 (1997) 303.
[3] J.C. Yori, C.L. Pieck and J.M. Parera, Appl. Catal. 181 (1999) 5.
[4] M.J. Ledoux, P.D. Gallo, C.P. Huu and A.P.E. York, Catal. Today 27 (1996) 145.
[5] J.K. Lee and H.K. Rhee, in: *Zeolite Science 1994: Recent Progress and Discussions Studies in Surface Science and Catalysis*, Vol. 98, eds. H.G. Karge and J. Weitkamp (Elsevier, Amsterdam, 1995) p. 169.
[6] A.P.E. York, P.H. Cuong, P.D. Gallo and M.J. Ledoux, Catal. Today 35 (1997) 51.
[7] K.I. Patrylak, F.M. Babonych, Yu.G. Voloshyna, M.M. Levchuk, V.G. Il'in, O.M. Yakovenko, I.A. Manza and I.M. Tsupryk, Appl. Catal. 174 (1998) 187.
[8] A. Chica and A. Corma, J. Catal. 187 (1999) 167.
[9] J.A. Moreno and G. Poncelet, Appl. Catal. 210 (2001) 151.
[10] S. Kuba, B.C. Gates, R.K. Grasselli and H Knözinger, Chem. Commun. 321 (2001).
[11] R.M. Jao, T.B. Lin and J.R. Chang, J. Catal. 161 (1996) 222.
[12] F. Babou, G. Coudurier and J.C. Védrine, J. Chim. Phys. 92 (1995) 1457.
[13] J.M. Campelo, F. Lafont and J.M. Marinas, Zeolites 15 (1995) 97.
[14] S. Kuba, P.C. Heydorn, R.K. Grasselli, B.C. Gates, M. Che and H. Knözinger, Phys. Chem. Chem. Phys. 3 (2001) 146.
[15] S. Ardizzone and C.L. Bianchi, Appl. Surf. Sci. 152 (1999) 63.
[16] E. Baburek and J. Nováková, Appl. Catal. 185 (1999) 123.
[17] S. Rezgui, A. Ghorbel and B.C. Gates, J. Chim. Phys. 92 (1995) 1576.
[18] C. Perego and P. Villa, Catal. Today 34 (1997) 281.
[19] R.D. Gonzalez, T. Lopez and R. Gomez, Catal. Today 35 (1997) 293.
[20] M. Signoretto, M. Scarpa, F. Pinna, G. Strukul, P. Canton and A. Benedetti, J. Non-Cryst. Solids 225 (1998) 178.
[21] M. Hino and K. Arata, Appl. Catal. 169 (1998) 151.
[22] G.P. Babu and R.S. Murthy, in: *Recent Developments in Catalysis Theory and Practice*, eds. B. Viswanathan and C.N. Pillai (Editions Technip, Paris, 1992) p.450.
[23] J.F. Lepage, in: *Catalyse de contact* (Editions Technip, Paris, 1978) p. 430.
[24] S. Bendezu, R. Cid, J.L.G. Fierro and A.L. Agudo, Appl. Catal. 197 (2000) 47.
[25] A. Katrib, V. Logie, N. Saurel, P. Wehrer, L. Hilaire and G. Maire, Surf. Sci. 377–379 (1997) 754.
[26] A. Katrib, V. Logie, M. Peter, P. Wehrer, L. Hilaire and G. Maire, J. Chim. Phys. 94 (1997) 1923.
[27] C. Bigey, L. Hilaire and G. Maire, J. Catal. 184 (1999) 406.
[28] C. Bigey, L. Hilaire and G. Maire, J. Catal. 198 (2001) 208.
[29] G. Larsen and L.M. Petkovic, Appl. Catal. 148 (1996) 155.
[30] M.G. Falco, S.A. Canavese, R.A. Comelli and N.S. Figoli, Appl. Catal. 201 (2000) 37.
[31] J.C. Yori and J.M. Parera, Appl. Catal. 129 (1995) 83.
[32] T. Matsuda, H. Sakagami and N. Takahashi, J. Chem. Soc. Faraday Trans. 93 (1997) 2225.
[33] M. Pérez, H. Armendariz, J.A. Toledo, A. Vasquez, J. Navarrete, A. Montoya and A. Garcia, J. Mol. Catal. 149 (1999) 169.
[34] D. Ouafi, F. Mauge, J.C. Lavalley, E. Payen, S. Kasztalan, M. Houari, J. Grimblot and J.P. Bonnelle, Catal. Today 4 (1988) 23.
[35] V.M. Benitez, C.A. Querini, N.S. Figoli and R.A. Comelli, Appl. Catal. 178 (1999) 205.

[36] A. Katrib, F. Hemming, P. Wehrer, L. Hilaire and G. Maire, J. Elect. Spect. Relat. Phenom. 76 (1995) 195.
[37] D.G. Barton, S.L. Soled, G.D. Meitzner, G.A. Fuentes and E. Iglesia, J. Catal. 181 (1999) 57.
[38] K. Shimizu, T.N. Venkatraman and W. Song, Appl. Catal. 224 (2002) 77.
[39] Z.R. Finelli, N.S. Figoli and R.A. Comelli, Catal. Lett. 51 (1998) 223.
[40] E. Iglesia, D.G. Barton, J.A. Biscardi, M.J.L. Gines and S.L. Soled, Catal. Today 38 (1997) 339.
[41] S.A. Vaudagna, R.A. Comelli and N.S. Figoli, Appl. Catal. 164 (1997) 265.
[42] S. Meijers, L.H. Gielgens and V. Ponec, J. Catal. 156 (1995) 147.
[43] S.L. Soled, G.B. McVicker, L.L. Murrell, L.G. Sherman, N.C. Dispenziere, S.L. Hsu and D. Waldman, J. Catal. 111 (1988) 286.
[44] B. Parlitz, E. Schreier, H.L. Zubowa, R. Eckelt, E. Lieske, G. Lieske and R. Fricke, J. Catal. 155 (1995) 1.
[45] K. Chao, H. Wu and L. Leu, Appl. Catal. 143 (1996) 223.